JOURNAL OF MATERIALS SCIENCE 17 (1982) 1700–1712

Crystalline state extrusion of high-density polyethylene as a function of die entrance angle

WILLIAM G. PERKINS*, ROGER S. PORTER
Polymer Science and Engineering Department, Materials Research Laboratory, University of Massachusetts, Amherst, Massachusetts 01003, USA

High-density polyethylene (HDPE) of two different average molecular weights, $\bar{M}_w$, has been solid-state extruded in an Instron capillary rheometer through brass capillary dies of several entrance angles from 10 to 180°. Extrusion rates increase substantially at smaller angles whereas the maximum achievable extrusion draw ratio, (R_E), is realized at larger angles. At a constant R_E, maxima are observed in plots of linear expansion coefficient, Young's modulus, tensile strength and elongation at break against die entrance angle. These maxima occur at angles of 20 to 30° for the lower molecular weight HDPE ($\bar{M}_w$ = 59 000). For the higher molecular weight HDPE ($\bar{M}_w$ = 92 000) maxima were at angles of 14 to 20°.

1. Introduction

Ultra-oriented high-density polyethylene (HDPE) films and fibres have been produced in this laboratory by solid (crystalline) state extrusion using an Instron capillary rheometer [1]. A typical die is of brass with a 20° included entrance angle, 2α, and a nominal extrusion draw ratio of 50. However, actual extrusion ratios on samples are generally less. This is because the total volume of polymer initially in the tapered die entrance region is not extruded before the extrudate fractures. This means that the maximum potential extrusion draw can be difficult to achieve. This study is an attempt to clarify the importance and efficiency of the capillary die entrance angle with respect to extrusion characteristics and physical properties of the extrudates for HDPE.

In even a qualitative analysis of the deformation undergone by the polymer in solid-state extrusion, one must consider both the shear and extensional forces and flows occurring within the die entrance region. Such discussions in the literature are liminted to melt flow so that such results are considered here only as analogous to solid-state flow. Under the high extrusion pressures commonly encountered in the process ($\leqslant$ 0.49 GPa), consideration must also be given the effect of pressure on the transitions and yield properties of extruded polymers.

According to Cogswell [2] for melt flow, "simple shear deformation takes place when the flow streamlines are parallel, but correspond to different material velocities". This corresponds to entrances having small angles, which in the geometrical limit, as 2α approaches zero, are straight tubes. Cogswell continues, "extensional flow occurs when the streamlines through a cross-section corrspond to constant material velocities, but are not parallel". This is the case involving larger entrance angles, which in a limit would be 180°, i.e., a square entrance region. In his review on the processing of ultra-high modulus polymers, Bigg [3] states than an elongational velocity gradient is needed to develop the necessary molecular structure for superior extrudate physical properties. He speculates that small entrance angles most probably cannot produce such a gradient. On the other hand, Bigg goes on to say that a uniform elongational velocity gradient is difficult to realize at large die angles, because of localized high elongation of the material at the entrance to the capillary portion of the die.

Although a well-developed elongational velocity gradient is seen as important for the enhancement

*Present address: The Goodyear Tire and Rubber Company, Akron, Ohio, USA.

0022–2461/82/061700–13$04.06/0

of extrudate physical properties, excessively high extensional stresses are believed to cause gross extrudate fracture [4, 5]. Shaw [4] postulates that lubrication of the die energy region minimizes or eliminates shear stresses, thus generating high extensional stresses which result in melt fracture. A balance of shear and extensional deformation was also seen as important by Predecki and Statton [6] who noted that die lubrication reduced the efficiency of the molecular orientation process by reducing shear stresses. Everage and Ballman [5] calculated a critical recoverable extensional strain, and state that once this strain is attained, the material cannot elastically deform fast enough to reach a steady-state extensional stress level, and fracture may result. They conclude that melt fracture can be a consequence of tensile failure of the material in extensional deformation. Metzger *et al.* [7], show that the magnitude of the shear stresses developed during melt extrusion of HDPE is proportional to the molecular weight. From the calculations of Cogswell relating extensional and shear stresses to entrance angle, one would expect smaller extensional stresses at larger entrance angles. This means a higher extrusion ratio before fracture should be possible for higher molecular weight materials extruded through larger entrance angles. This would appear to be the case for the Nakayama and Kanetsuna study [8] on hydrostatic extrusion of HDPE where the optimum entrance angle (lowest extrusion pressure required) was found to be 60°, at a HDPE molecular weight twice as high as the Alathon 7050 used in this study. Imada and Takayanagi [9], processing HDPE via solid-state extrusion, found the optimum included entrance angle to be 20 to 40°, using a HDPE having approximately the same molecular weight as the Alathon 7050 used here.

Pugh [10] believes that two important factors influence the choice of optimum die entrance angle. One is the "redundant work", caused by shearing of the material as it enters the deformation (entrance) zone and flows toward the die orifice. This factor increases with increasing die angle. The other factor is the frictional work at the polymer billet–die interface. This decreases with increasing die angle. Pugh concludes that there would quite naturally be a minimum in the relationship between extrusion pressure and die angle. He further observed that this minimum shifts toward smaller angles as the coefficient of friction between the billet material and the die decreases.

The effect of pressure on the mechanical properties of polymers must be considered in an analysis of solid-state extrusion since the material being extruded is under high pressure in both the die and rheometer barrel. It is generally concluded that both the modulus and yield stress rise substantially with increasing hydrostatic pressure [11, 12]. Ainbinder *et al.* [13], attribute the modulus increase at 2000 atm to a decrease in specific volume, analogous to cooling the polymer $> 100°$ C. They further state that the nature of the deformation of crystalline polymers in the presence of (all around) compression depends on the per cent crystallinity. For highly crystalline polymers (such as HDPE), the deformational process cannot be very dependent on conformational movements such as trans–gauche transformations, since mobility is restricted. The decisive factor will therefore be the extent of deformation. Since, the material undergoes less total deformation in large entrance angle dies (smaller entry volume), one might conclude that shear stress build-up will be less and maximum extrusion ratios higher.

Pae *et al.* [14], believe, from the behaviour of polyethylene single crystals, that bulk polymer under hydrostatic pressure will principally deform via shear modes. If this is indeed the case, die angles which reduce such stresses will allow larger deformations without fracture; they are larger angles. As stated by Mears *et al.* [11], under high pressure a higher applied pressure is required to initiate the molecular mobility associated with plastic yielding. This is because, as the material is compressed, the free volume is reduced and the seondary forces between neighbouring segments are therefore increased. This agrees with the general contention that yield stress increases with high pressure and strain-to-fracture decreases during tensile tests in a high-pressure environment. Therefore, the higher pressures necessary for solid-state extrusion are also responsible for the ultimate failing of the extrudate at high extrusion ratios. From the data of Mears *et al.* [11], and Ward *et al.* [12], the tensile stress increases more rapidly with increasing pressure than does the shear yield stress. Therefore, larger entrance angles, where shear stresses (not strains) are larger, should allow attainment of greater extrusion ratios.

2. Experimental procedure

The high-denisty polyethylenes used exclusively in this study were DuPont Alathons 7050 ($\bar{M}_n$:

59 000; $\bar{M}_n$:19 900) and 7030 ($\bar{M}_w$:92 000; $\bar{M}_w$: 26 000) [15]. They were extruded through brass capillary dies having entrance angles of 10, 14, 20, 30, 60, 90, 120 and 180° (see Fig. 1). A 6° entrance angle die was also tested, but with anomalous results, and subsequent inspection of the die revealed faulty die machining, so these results were not included.

The capillary length for all entrance angles was 1.0 cm and the diameter was 0.132 cm. The original billet diameter was 0.95 cm. Extrusions were undertaken at 0.247 GPa pressure and 134° C. Teflon film-bonding grade lubricant was sprayed on the highly polished dies prior to extrusion. The solid-state extrusion technique was as previously described [1], except that no weight was attached to the emerging extrudates, which were instead extruded through a glass tube to insure straightness. The extrusion rate at each entrance angle was measured with a cathetometer under steady-state conditions. Characterization techniques applied to the extrudate included differential scanning calorimetry, bi-refringence, thermomechanical analysis and mechanical testing.

Differential scanning calorimetry (DSC) was performed with a Perkin–Elmer DSC-1B differential scanning calorimeter at a heating rate of 10° C min^{-1} to yield heat of fusion (converted to per cent crystallinity) and crystalline melting points. The heat of fusion for a perfect crystal was taken as 5.02×10^5 J kg^{-1}.

Bi-refringence measurements were carried out on a Zeiss polarizing microscope equipped with an Ehringhaus rotary compensator consisting of double calcite plates. The compensator can measure up to 133 orders of retardation in white light. The magnitude of the bi-refringence was calculated from

$$\Delta = \frac{\delta\lambda}{t}, \qquad (1)$$

where Δ is the total bi-refringence of the fibre,

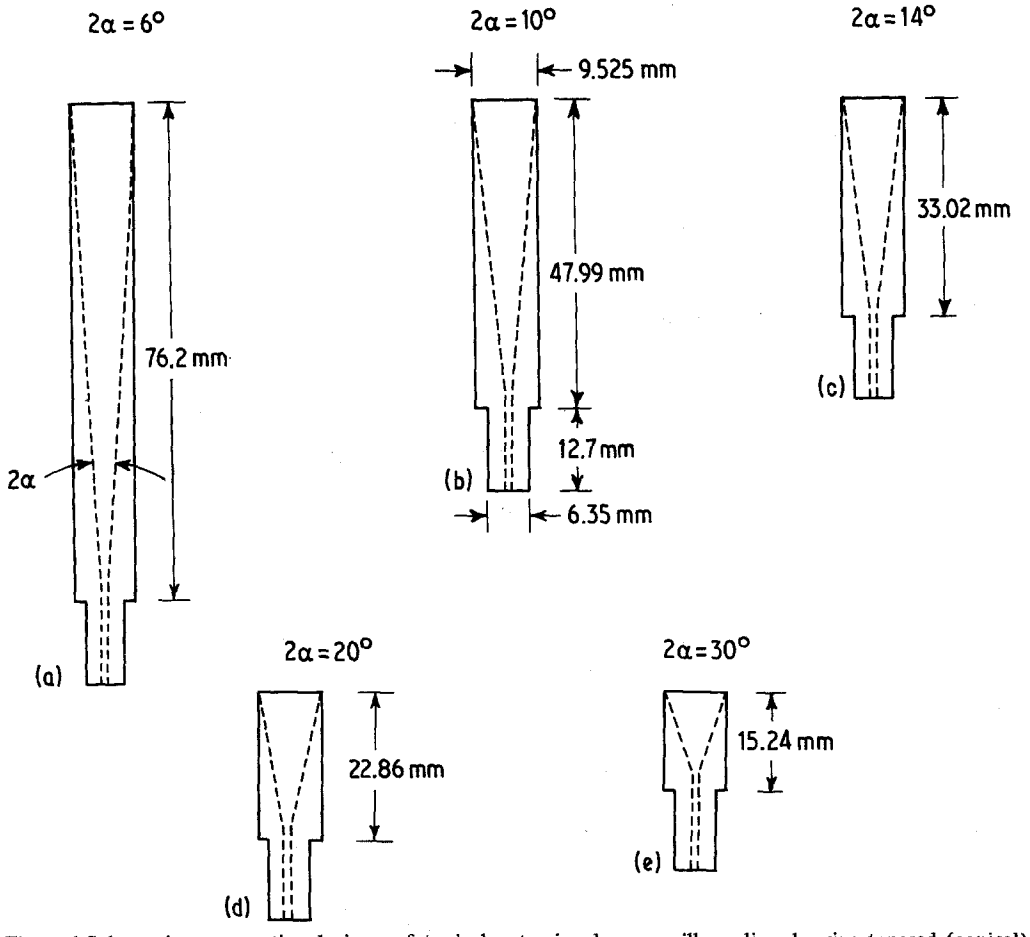

Figure 1 Schematic cross-sectional views of typical extrusion brass capillary dies showing tapered (conical) entrance region and relative volumes.

δ is the retardance, λ is the wavelength of white light (567.4 nm), and t is the fibre thickness (diameter).

A Perkin–Elmer TMS-1 thermomechanical analyser attachment to the DSC-1B machine was used for measurement of the linear expansion coefficient, α, as well as the thermal transitions. Sample preparation for this test was as previously described [16]. A small load of 3 g was used with the expansion probe, and the scanning rate was 10° C min^{-1}. The test sample length was approximately 1 cm. Scans were made from -110 up to 120° C.

For studies of mechanical properties on extruded fibres, an Instron tensile testing machine, model TTCM, was used, equipped with a strain-gauge extensometer. Load–elongation curves were obtained at room temperature using a fixed elongation rate of 0.02 cm min^{-1} for accurate modulus measurements, and 0.50 cm min^{-1} for determination of tensile strength and strain-at-break. The fibres had to be gripped by special clamps described elsewhere [17] to prevent slippage in the jaws. The Young's modulus was determined as the tangent to the stress–strain curve at 0.1 % strain.

3. Results

3.1. Extrusion rate

The rate of extrusion for HDPE (Alathon 7050) plotted against die entrance angle is shown in Fig. 2. The steady-state rate decreases rapidly from 1.16 cm min^{-1} at the 10° entrance angle to 0.2 cm min^{-1} at an entrance angle of 120°. At still larger angles, the rate remains fairly constant at about 0.2 cm min^{-1}. For Alathon 7030 ($\bar{M}_w$: 92 000), the extrusion rates, although generally slower, behave similarly. They decrease from 0.43 cm min^{-1} at the 10° entrance angle to 0.072 cm min^{-1} at 120°, thereafter remaining nearly constant. These steady-state extrusion rates appear well before the entrance cone volume is expended.

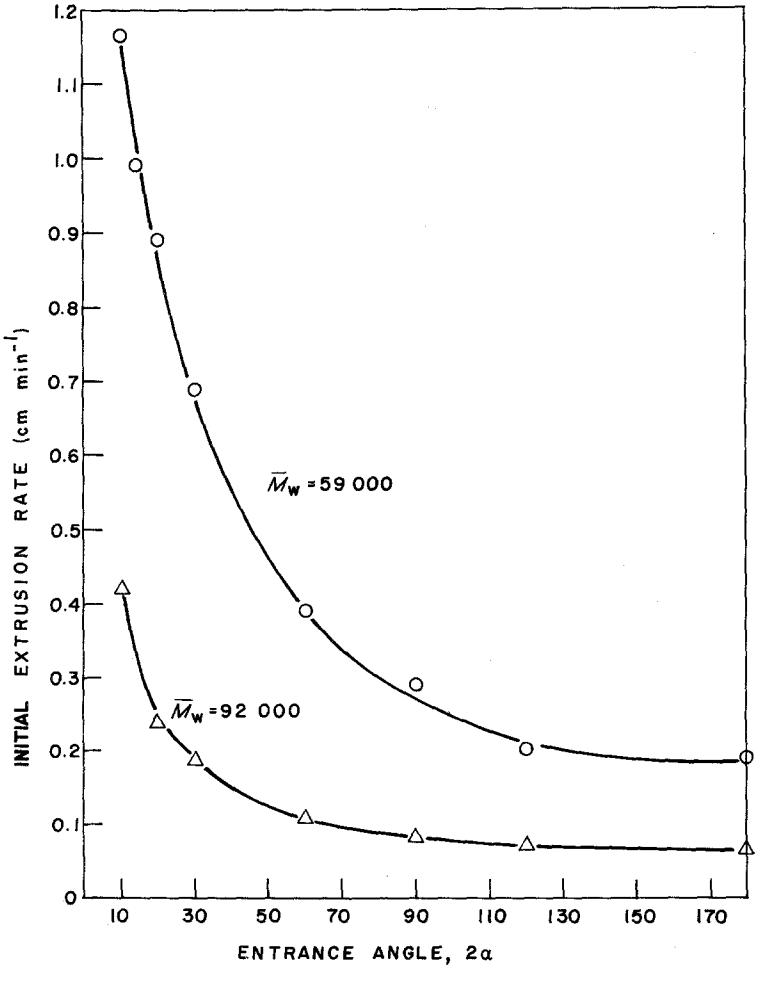

Figure 2 Extrusion rate plotted against die entrance angle for two HDPE polymers; $\bar{M}_w$ values as shown.

3.2. Deformation intensity

The concept of deformation intensity was developed in a paper by Capiati *et al.* [1] and plotted as a function of extrusion draw ratio. Deformation intensity, I_D, is defined as the rate of change of draw, which reaches a maximum at the entrance cone exit

$$\frac{d(R_E)}{dH}|_{max} = 2R_a^2 \frac{\tan \alpha}{R_b^3}, \quad (2)$$

where $dR_E/dH|_{max}$ is the maximum deformation intensity, I_D, R_a is the rheometer barrel (reservoir) radius, R_b is the extrudate radius, α is the entrance cone semi-angle, H is the axial distance along the die and R_D is the extrusion (draw) ratio.

Fig. 3 is a plot of deformation intensity against entrance angle. It is seen that I_D rapidly increases with increasing entrance angle. According to Capiati *et al.* [1], the relationship between I_D and extensional shear rate is given by

$$\frac{dV}{dH} = V_a \frac{dR_E}{dH}, \quad (3)$$

where V and V_a are material velocities at two points within the conical die entrance region. Since the extensional shear rate is shown above to be proportional to I_D, and present data show I_D to increase with larger entrance angles, one can conclude that extensional shear rates increase with increasing entrance angles. This indicates a more efficient molecular extension at larger angles and higher ultimate extrusion ratios would be expected at the larger angles.

3.3. Extrusion length at fracture

The curves showing extrusion length at fracture against entrance angle shown in Fig. 4 are similar to those of extrusion rate against entrance angle. A rapid decrease in maximum extrudate length from 10° to 60° is followed by a more gradual decrease at larger angles. The two molecular-weight curves cross at a projected entrance angle of 85°. The 14° data for the lower molecular weight Alathon 7050 is anomalously low and may be due to a less well polished die.

3.4. Maximum extrusion ratio

The maximum extrusion draw ratio, R_E, obtainable is plotted as extrusion ratio-at-fracture against die entrance angle in Fig. 5. These data mark the

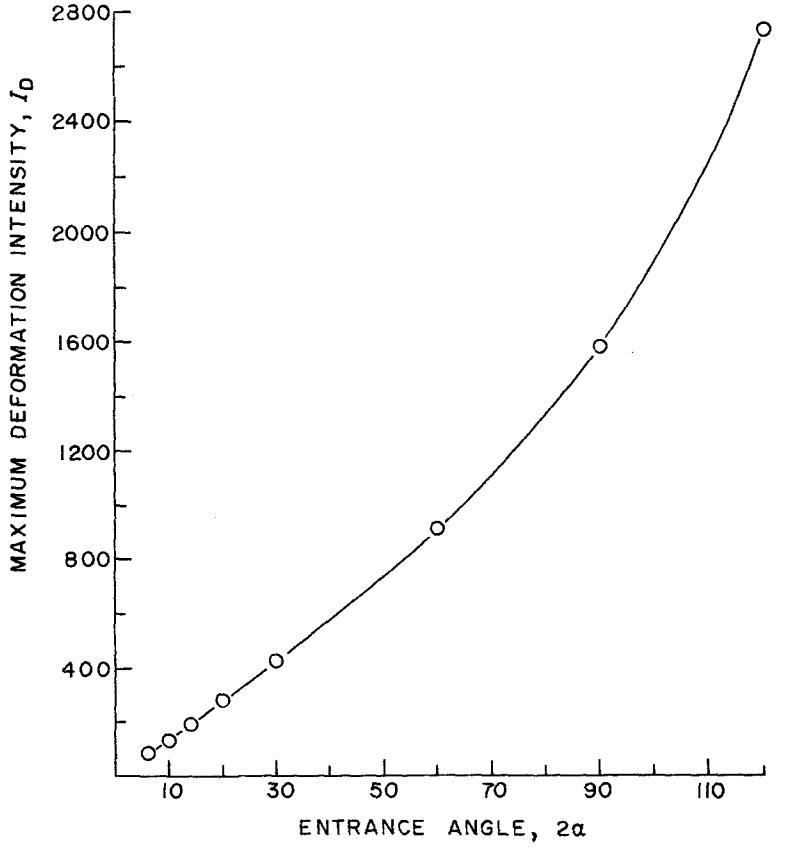

Figure 3 Maximum deformation intensity plotted against die entrance angle, see Equation 1.

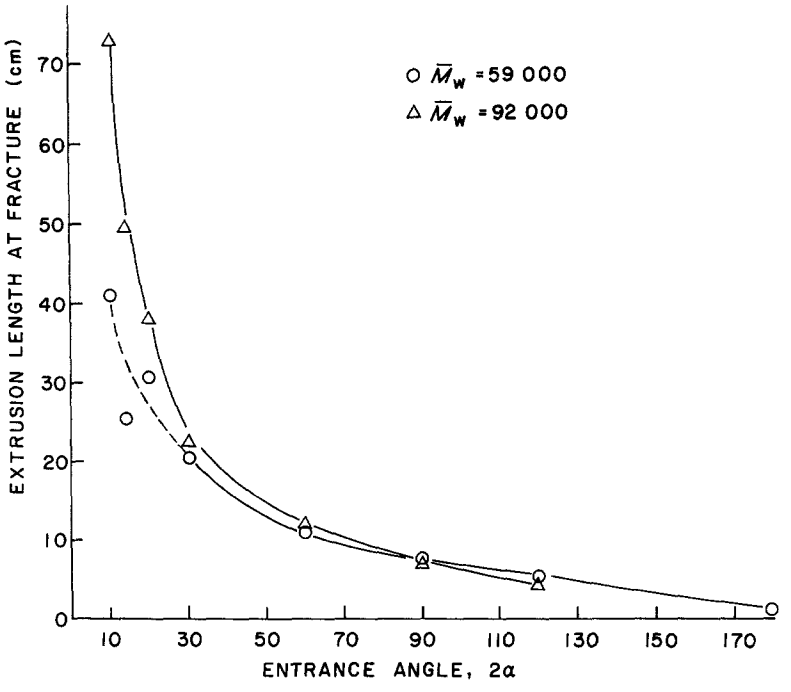

Figure 4 Maximum extrusion length prior to fracture plotted against die entrance angle for two HDPE polymers; $\bar{M}_w$ values as shown.

points where extrudate fracture (manifested by crazes oriented at 20 to 30° to the extrusion direction) began. The maximum R_E value possible with the dies used in this study was 52, found by dividing the cross-sectional area of the capillary exit into the cross-sectional area of the Instron rheometer barrel. This R_E value was realized with Alathon 7050 in the 120° entrance angle die. Lowering the entrance angle from 120° to 20° at this same molecular weight ($\bar{M}_w$:59 000) produced a linear decrease in the maximum obtainable R_E value. For strands extruded through dies having entrance angles less than 20°, fracture occurs at (even significantly) lower R_E values, as shown in Fig. 5. For the higher molecular weight Alathon 7030, the maximum obtainable R_E value of 49 also occurred with the 120° die. Maximum R_E values for this polymer decreases linearly from 49 at the 120° angle to 43.5 at the 10° entrance angle.

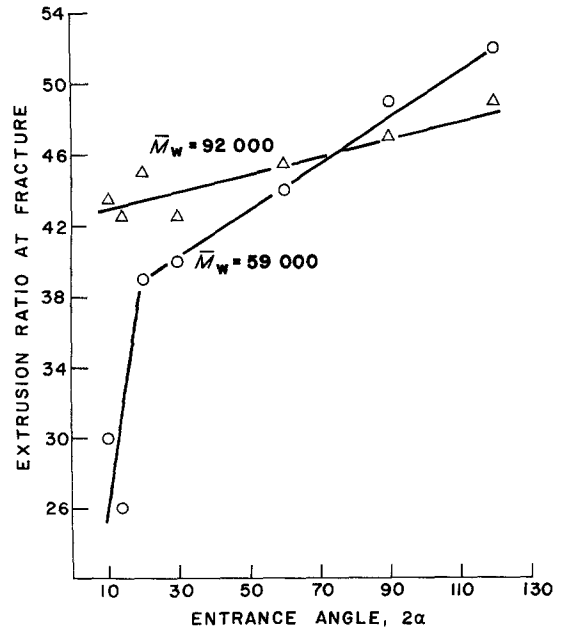

Figure 5 Extrusion ratio, R_E, at fracture plotted against die entrance angle for two HDPE polymers; $\bar{M}_w$ values as shown.

3.5. Bi-refringence

Bi-refringence, a measure of total (amorphous and crystalline) orientation, is plotted as a function of extrusion draw ratio in Figs 6 and 7 for all entrance angles. Fig. 6, a plot of bi-refringence against R_E curves for Alathon 7050, shows that all extrudates exhibit low orientation at low R_E values (of about 10) with the 120° strands quite low. At an R_E value of 20, orientation has increased, significantly for some angles, and to a lesser extent for others. Moving up to an R_E value of 24, where mechanical properties were measured, it can be seen that the 20, 30, 60 and 90° strands exhibit high orientation, whereas the 14 and the 120° strands remain of lower orientation. The curves appear to approach a limiting bi-refringence of 0.062. The 10° strands were not sufficiently transparent to allow bi-refringence measurements.

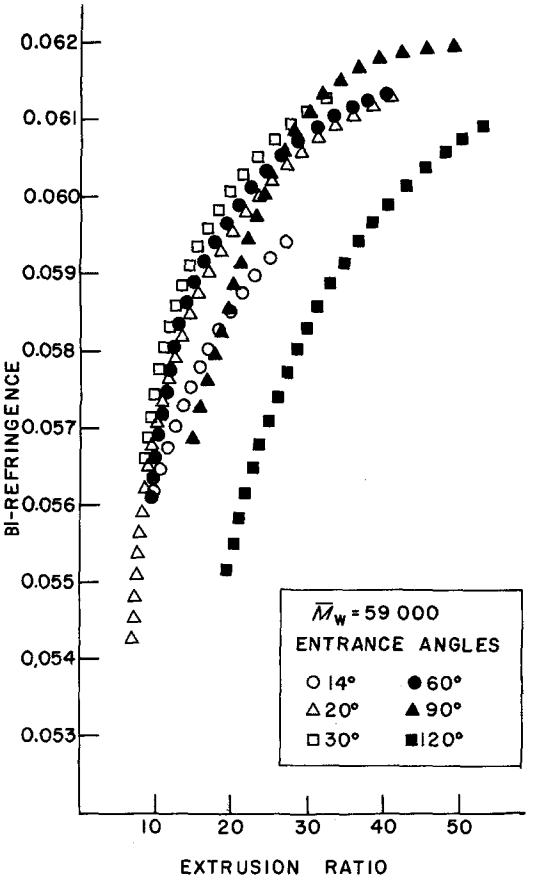

Figure 6 Bi-refringence plotted against ratio for Alathon 7050 HDPE extruded through dies of various entrance angles.

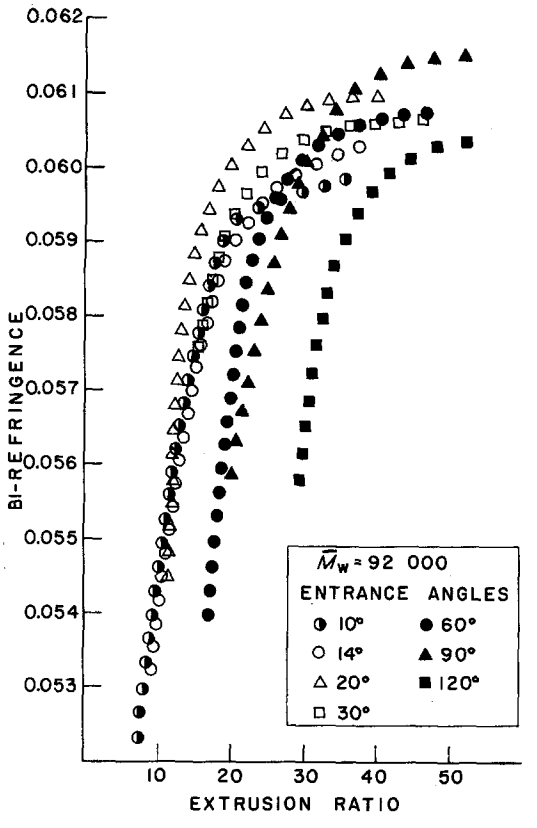

Figure 7 Bi-refringence plotted against extrusion ratio for Alathon 7030 HDPE extruded through dies of various entrance angles.

Fig. 7 is a plot of bi-refringence against R_E for the higher molecular weight Alathon 7030. At low extrusion ratios the values are lower than those of the Alathon 7050 resin. At an R_E value of 20, the 20° extrudates appear to be the most highly oriented, while others remain quite low. At an R_E value of 24, the 20 and 30° fibres show the highest orientation, while the 90 and 120° fibres remain least oriented. Except for the 90° extrudates, bi-refringence values for the 7030 fibres, with R_E greater than about 35, tend toward a limit of 0.061. Nakayama and Kanetsuna [8] found that X-ray (crystal) orientation was invariant with die entrance angle up to 90° while extrudates from the 120° die showed lower crystal orientation. Differences in the present results may then be due to amorphous phase orientation. The literature value calculated from maximum bi-refringence of a perfectly oriented HDPE crystal is 0.059 [18]. In this laboratory, Mead *et al.* [19] have observed a maximum bi-refringence of ultra-oriented HDPE of 0.062.

TABLE I Crystalline melting points and per cent crystallinities for Alathon 7050 solid-state extruded at $R_E = 10$.

Entrance angle (°)	Crystalline melting point, (° C)	Crystallinity (%)
10	136.3	77.5
14	135.8	78.5
20	136.0	79.5
30	136.0	79.5
60	136.3	81.5
90	136.0	78.0
120	135.0	74.5

TABLE II Crystalline melting points and per cent crystallities for Alathon 7030 solid-state extruded at $R_E = 10$.

Entrance angle (°)	Crystalline melting point, (° C)	Crystallinity (%)
10	137.5	71.0
14	138.3	72.0
20	137.0	72.0
30	138.0	71.0
60	137.5	71.3
90	137.7	71.0
120	136.8	68.3

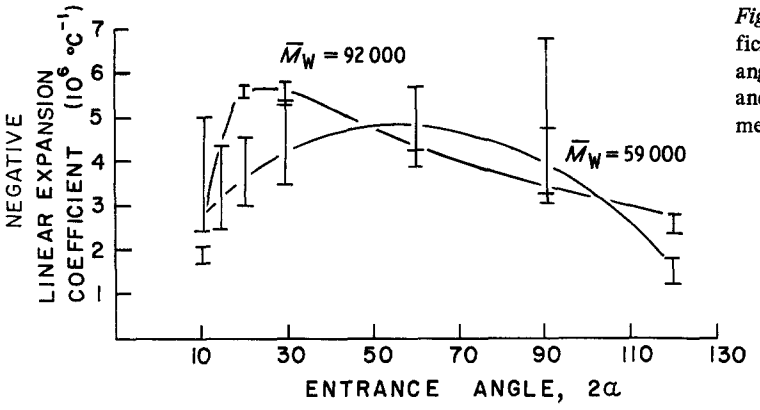

Figure 8 Negative linear expansion coefficient plotted against die entrance angle for Alathon 7050 HDPE and Alathon 7030 HDPE. Measurements made at $E_R = 20$.

3.6. Calorimetry

Differential scanning calorimetry (DSC) results for crystalline melting-point and per cent crystallinity of the two molecular weight HDPEs are shown in Tables I and II. Measurements were made at an R_E value of 10. The fibres extruded through the 120° die have the lowest melting point and per cent crystallinity. Strands extruded through dies at the other angles show no significant variation in melting point or per cent crystallinity.

3.7. Thermomechanical analysis

Thermomechanical analysis (TMA) yielded values of linear expansion coefficient, α, in the orientation direction over various temperature ranges. These coefficients, in $^\circ C^{-1}$, are obtainable from the slopes of plots of normalized sample length change against scanning temperature. Values of α_1, the coefficient measured from −110 to −80° for Alathon 7050 and measured from −110 to −73.5° for Alathon 7030, are plotted against die entrance angle in Fig. 8. These measurements were taken at an R_E value of 20. The data from Alathon 7050 showed a rather larger scatter, but appeared to show a maximum between the 30 and 90° entrance angle. The higher molecular-weight (Alathon 7030) data in Fig. 8 show an increase to a maximum at the 20 to 30° angles, then a gradual decline at larger angles.

3.8. Mechanical testing

Tensile properties were measured at an R_E value of 24. Stress–strain curves at low (0.1 %) strain resulted in the Young's modulus against die entrance angle values in Fig. 9 showing a maximum at die angles near 20° for the two molecular weights.

Tensile strength at break is plotted against die entrance angle in Fig. 10 which again exhibits a maximum near 20° for the two molecular weights. Values for the higher molecular-weight extrudates are generally higher than their lower molecular-weight counterparts.

Strains at break show a similar trend when plotted against die entrance angle in Fig. 11. Ulitimate properties of strands extruded through larger die entrance angles are difficult to obtain due to their short lengths and subsequent slippage in the testing machine grips. For this reason, some larger angle data is missing in these plots.

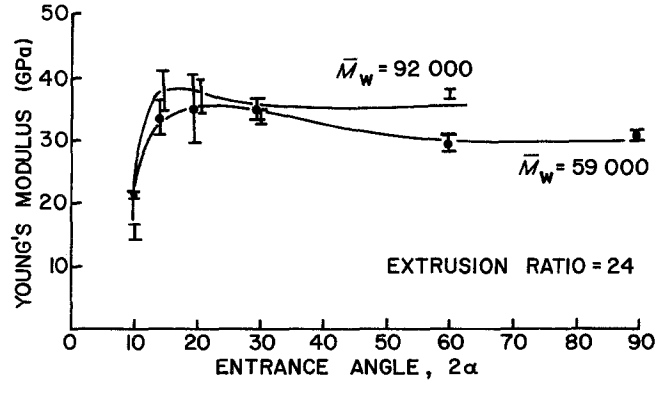

Figure 9 Young's modulus plotted against die entrance angle for Alathon 7050 HDPE and Alathon 7030 HDPE. Measurements made at $R_E = 24$.

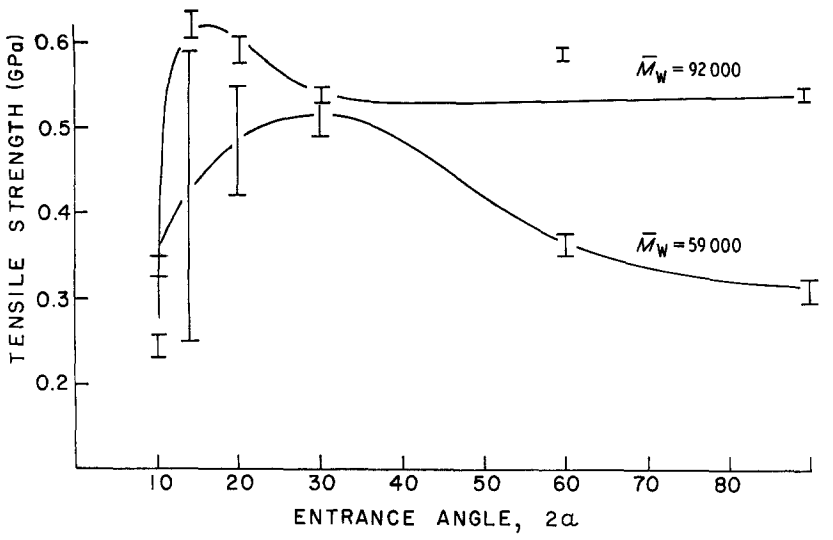

Figure 10 Tensile strength-at-break plotted against die entrance angle for Alathon 7050 HDPE and Alathon 7030 HDPE. Measurements made at R_E = 24.

Fig. 12 shows schematically two types of load-cycling curves obtained during low strain mechanical tests at an elongation rate of 0.02 cm min^{-1}. Curve a is typical for fibres extruded through the die with the 10° entrance region, whereas Curve b is typical for fibres extruded through all higher angles and for both molecular weights. The area within a given (open) loop is a measure of the energy dissipated, E_d, for that particular cycle. A plot of E_d against die entrance angle is shown in Fig. 13. The data for both molecular weights fall on the same curve. There is a drop from the 10° entrance angle to the 14° angle, followed by a plateau, followed by a slow rise at higher angles.

Fig. 14 relates the energy dissipated to Young's modulus for strands at an R_E value of 24. The data for both molecular weights fall on the same curve. It is seen that there is an inverse relationship between the energy dissipated in a stress–strain cycle and Young's modulus which is more pronounced at lower moduli. The unusually high E_d values for the Alathon 7030 extrudate at low Young's moduli correspond to extrudates formed by the 10° entrance angle die.

4. Discussion and conclusions

4.1. Extrusion rate

The results of the extrusion rate data, plotted in Fig. 2, indicate that the deformation process is facilitated by a streamlined (more gradually tapered) entrance region, at least up to angles of 120°. As the entrance angles tend toward 0°,

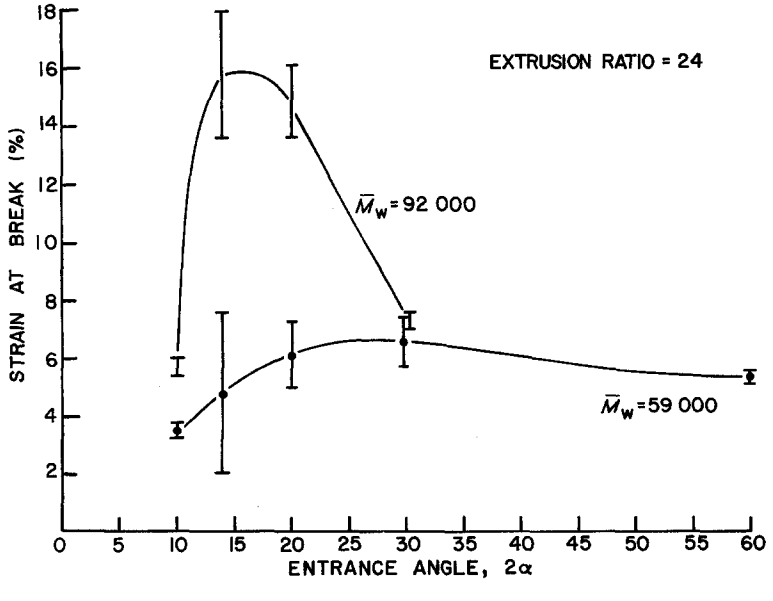

Figure 11 Strain-at-break plotted against die entrance angle for Alathon 7050 HDPE and Alathon 7030 HDPE. Measurements made at R_E = 24.

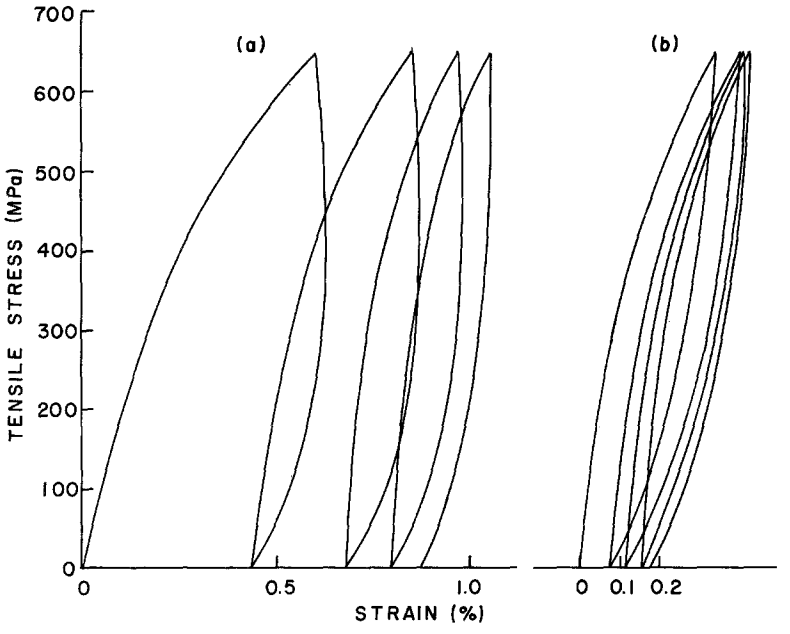

Figure 12 Strain-cycling curves at an elongation rate of 0.02 cm min^{-1} for (a) HDPE extruded through a 10° entrance angle die and (b) HDPE extruded through dies of all other angles.

the extrusion rates tend toward very high values. This would be expected as the deformation becomes increasingly parallel to the primary compressive force applied by the Instron plunger. However, although these smaller angles result in faster extrusion rates and longer extrudates, the actual maximum extrusion ratio attainable increases with increasing entrance angle. This indicates that a large extensional component is necessary for optimum crystalline state deformation efficiency. This occurs with larger entrance angles.

4.2. Extrusion length and extrusion ratio at fracture

The curves of maximum extrusion length against entrance angle cross at a projected angle of 85°. At smaller angels, the higher molecular-weight Alathon 7050 produces longer extrudates, while at larger (> 85°) angles, both molecular weights produce approximately equal lengths at a given angle. There is an unexplained low value in the curve for Alathon 7050 at an entrance angle of 14°. The extrusion ratio at fracture against entrance angle curves for the two molecular weights also cross at the projected 85° die angle. Below this angle the higher molecular weight HDPE allows attainment of greater extrusion ratios, whereas above the cross-over point, the lower molecular weight HDPE results in fibres having greater maximum R_E values. Both maximum extrusion length and extrusion ratio results indicate that the cold extrusion process is more efficient at smaller entrance angles for higher molecular weight HDPE and more efficient at larger entrance angles for lower molecular weigth HDPE. Possibly, the two curves in Figs 4 and 5 cross because the higher molecular weight HDPE cannot utilize effectively

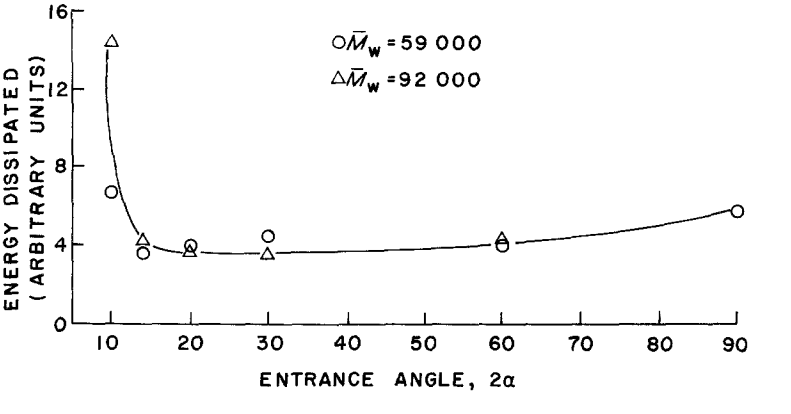

Figure 13 Energy dissipated plotted against Young's modulus for two HDPE polymers; $\bar{M}_w$ values as shown. For explanation see text.

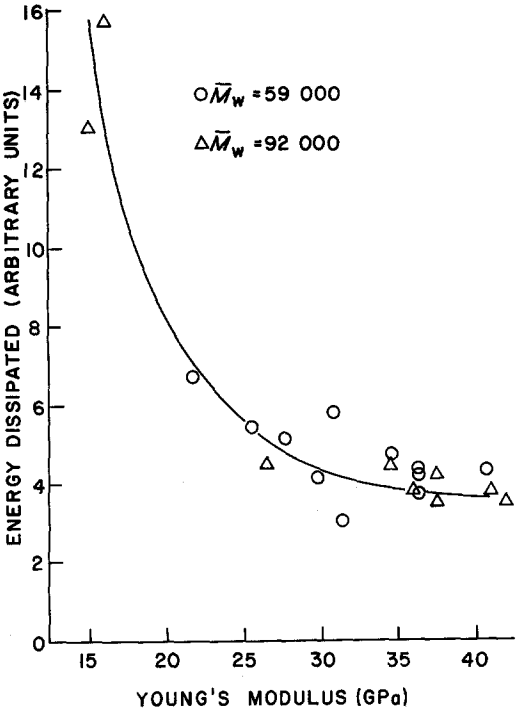

Figure 14 Energy dissipated plotted against Young's modulus for two HDPE polymers; $\bar{M}_w$ values as shown. For explanation see text.

the high elongational deformation taking place at the larger entrance angles while the lower molecular weight HDPE is not deformed efficiently at the smaller angles.

4.3. Bi-refringence

Bi-refringence measurements indicate that greater total orientation is achieved for the lower molecular weight fibres at any given extrusion ratio and entrance angles greater than 20°. The 20° entrance angle curves for HDPEs cross at an extrusion ratio of 12 and also at 35 for the higher molecular weight strands, whereas the 14° curve for the higher molecular weight strands show greater bi-refringence above an R_E of 15. Again, the deformation process for the lower molecular weight HDPE appears more efficient at large entrance angles while for the higher molecular weight HDPE, smaller entrance angles seem to be more advantageous. At the 120° entrance angle, both molecular weights give poorly oriented extrudates. This could result from annealing of the extrudate in the die as it emerges at the slow rates characteristic of high angles.

4.4. Calorimetry

Measurement of crystalline melting point and per cent crystallinity indicates that no great change in crystal size and/or perfection results from altering the die entrance angle except at an angle of 120°, where the crystal quality is apparently lower at an R_E value of 10. This is probably due to the lower total orientation of fibres extruded through this die, as shown by bi-refringence measurements. The melting points and crystallinity for the Alathon 7050 fibres are slightly higher in the 20 to 60° die entrance angle range, whereas those in the 14 to 30 die entrance angle range are higher for the higher molecular weight Alathon 7030 strands. These differences, however, border on the range of experimental error.

4.5. Coefficient of expansion

The magnitude of the negative linear expansion coefficient in the orientation direction is a qualitative measure of the extent of chain extension in ultra-oriented systems [15]. The results in this study suggest that maximum chain extension occurs in fibres extruded through the middle angle (30 to 90°) dies for Alathon 7050 and through the smaller angle (20 to 30°) dies for the higher molecular weight Alathon 7030. Both the 10° and 120° entrance angle fibres exhibited notable positive expansion coefficients in orientation direction shortly before the melting range. This indicates that the extended-chain crystals in these extrudates are somewhat unstable.

Possibly there is a relaxation (annealing) of the ultra-oriented morphology during extrusion. Such annealing would increase with slower extrusion rates (larger angles) and result in lower fibre orientation. This would explain why the high molecular-weight HDPE shows a maximum deformation efficiency at smaller angles than the lower molecular weight HDPE. For a given molecular weight, the extrusion rate is faster the smaller the angle. This phenomenon is competing with the present contention that larger angles result in more efficient deformation.

4.6. Mechanical testing

Curves of Young's modulus, tensile stress-at-break, and tensile strain-at-break, each plotted against die entrance angle, all show a similar trend. There is a maximum at die entrance angle of 20 to 30° for the lower molecular weight strands followed by a decrease and levellimg-off. For the higher

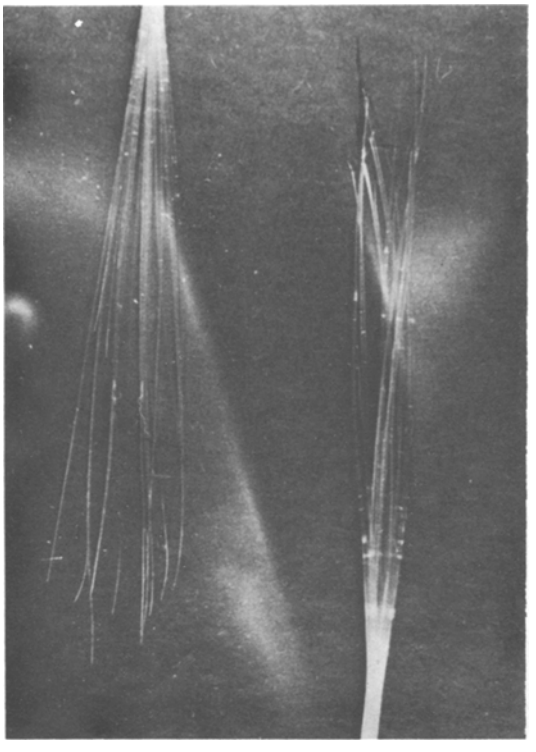

Figure 15 Unmagnified tensile fracture surface of typical solid-state extruded HDPE film.

molecular weight strands, the curve is similar except the maximum occurs at an angle of 14 to 20°.

These data imply that the overall efficiency of the solid-state deformation process depends on the molecular weight of the polymer as well as the capillary die entrance angle. Higher molecular weight polyethylene should be extruded through a smaller entrance angle die than lower molecular weight material if maximum deformation efficiency and physical properties are to be realized. A fibrillar fracture is observed on tensile testing to failure (Fig. 15) and the load–elongation curves show that fibrils comprising the strands fracture in stages as opposed to all breaking at once. The fibrillar morphology is shown at high magnification in Fig. 16. This is a scanning electron micrograph of ultra-oriented HDPE fractured along the orientation direction (horizontal in Fig. 16).

4.7. Elastic hysteresis

The elastic hysteresis, or energy dissipated through viscous heating during the stress–strain cycle, is a measure of elasticity. Smaller values imply a more highly elastic material, while larger values indicate a more viscous material with consequently poorer tensile properties. The hysteresis curves in Fig. 12 indicate that the fibres extruded through the 10° entrance angle (Curve a) are less elastic than the strands extruded through other dies. The plot of energy dissipated against die entrance angle (Fig. 13) shows that the 14, 20 and 30° entrance angles produce the most elastic extrudates followed by the 60, 90 and finally 10° angles. The relationship between dissipated energy and Young's modulus is shown in Fig. 14 where one sees an

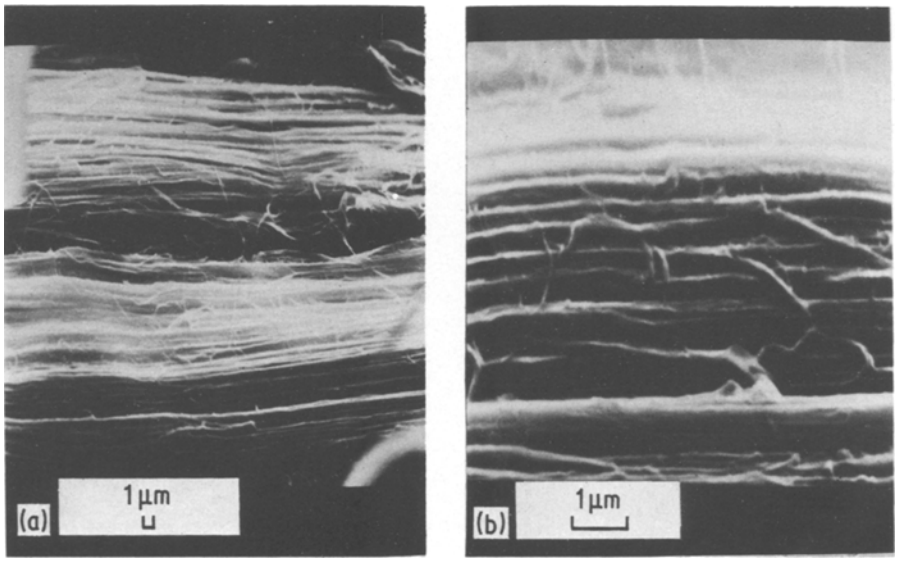

Figure 16 Typical fracture surfaces of solid-state extruded HDPE, peeled under liquid nitrogen. Two magnifications shown.

inverse relationship between the two parameters. Higher modulus materials, which by definition exhibit greater elasticity at small strains, dissipate less energy during strain cycling. The Young's moduli reported herein were measured as the tangent to the fifth-cycle hysteresis curve which produces the limiting increase in tensile modulus. Such modulus increase results from what is essentially further drawing during this cycling.

5. Conclusions

Optimum entrance angles for capillary dies used in solid state extrusion for HDPE vary with molecular weight. Other considerations such as extrusion temperature and type of polymer may well be equally important, as they may dictate the limiting shear and extensional stresses that the material can withstand before failing. A balance of shear and extensional forces is seen as important for the efficient deformation and chain unfolding necessary for high extrusion ratios and, thus, superior physical properties. The optimum condition is one where extensional strains are large and extensional stresses are minimized. However, shear forces must also be present for maximum deformation efficiency [5]. The actual entrance angle where these conditions exist will vary with the material being extruded and with the extrusion conditions. Ultimate extrusion ratios increase and extrusion rates decrease with larger entrance angles. Deformation efficiency, as measured by extrudate properties, is seen to increase at larger angles but is probably counteracted somewhat by annealing effects caused by the slower extrusion rates at large entrance angles.

Acknowledgement

The authors express appreciation to the Engineering Division of the National Science Foundation for support of this study.

References

1. N. J. CAPIATI, S. KOJIMA, W. G. PERKINS and R. S. PORTER, *J. Mater. Sci.* **12** (1977) 334.
2. F. N. COGSWELL, *Polymer Eng. Sci.* **12** (1972) 64.
3. D. M. BIGG, *ibid.* **16** (1976) 725.
4. M. T. SHAW, *J. Appl. Polymer Sci.* **19** (1975) 2811.
5. A. E. EVERAGE and R. L. BALLMAN, *ibid.* **18** (1974) 933.
6. P. PREDECKI and W. O. STATTON, *J. Polymer Sci. B*, **10** (1972) 87.
7. A. P. METZGER, C. W. HAMILTON and E. H. MERZ, *S.P.E. Trans.* January, (1963) 21.
8. K. NAKAYAMA and H. KANETSUNA, *Kobunshi Kagaku* **30** (1973) 713.
9. K. IMADA and M. TAKAYANAGI, *Int. J. Polymer Mater.* **2** (1973) 89.
10. H. LI. D. PUGH, (Ed) "Mechanical Properties of Materials Under Pressure", (Elsevier Publishing Co., Amsterdam New York and Oxford, 1970).
11. D. R. MEARS, K. D. PAE and J. A. SAUER, *J. Appl. Phys.* **40** (1969) 4229.
12. S. RABINOWITZ, I. M. WARD and S. S. C. PARRY, *J. Mater. Sci.* **5** (1970) 29.
13. S. B. AINBINDER, M. G. LAKA and I. Yu. MAJORS, *Mekhanika Polimerov* **1** (1965) 65.
14. K. D. PAE, D. R. MEARS and J. A. SAUER, *J. Polymer Sci. B*, **6** (1968) 773.
15. W. G. PERKINS, N. J. CAPIATI and R. S. PORTER, *Polymer Eng. Sci.* **16** (1976) 200.
16. R. S. PORTER, N. E. WEEKS, N. J. CAPIATI and R. J. KRZEWKI, *J. Therm. Anal.* **8** (1975) 547.
17. N. J. CAPIATI and R. S. PORTER, *J. Polymer Sci., Polymer Phys. Ed.* **13** (1975) 1177.
18. C. W. BUNN and R. DAUBENY, *Trans. Faraday Soc.* **50** (1954) 1173.
19. W. T. MEAD, C. R. DESPER and R. S. PORTER, *J. Polymer Sci., Polymer Phys. Ed.* **17** (1979) 859.

Received 24 September
and accepted 9 November 1981